Cement and Concrete Research 42 (2012) 937–944

Contents lists available at SciVerse ScienceDirect

Cement and Concrete Research

journal homepage: http://ees.elsevier.com/CEMCON/default.asp

Yield stress and bleeding of fresh cement pastes

A. Perrot [a], T. Lecompte [a], H. Khelifi [a], C. Brumaud [b], J. Hot [b], N. Roussel [b,*]

[a] Université de Bretagne Sud, LIMat B, Lorient, France
[b] Université Paris Est, IFSTTAR, Paris, France

ARTICLE INFO

Article history:
Received 22 April 2011
Accepted 19 March 2012

Keywords:
Rheology (A)
Bleeding (A)
Admixture (D)
Yield stress

ABSTRACT

We focus in this paper on a potential correlation between yield stress and bleeding. We suggest that the conditions under which a fresh cement paste is able to display a yield stress result from the competition between Brownian motion and colloidal interactions whereas the conditions under which the suspension is stable result from the competition between colloidal interactions and gravity. These competitions highly depend on the solid volume fraction of the system and on the polymer surface coverage. The correlation between yield stress and bleeding is therefore very indirect and difficult to use in practice.

1. Introduction

In the construction industry, a fluid concrete can only be called self-compacting concrete if its coarsest particles do not settle during casting and at rest before setting. At the scale of cement paste, a fluid cement paste is of practical interest only if it stays homogeneous despite the strong density difference between water and cement grains. This means that bleeding (i.e. the accumulation of water at the surface of the paste) of potentially usable fluid cement paste shall be neglectable (at least on a time scale of a few hours before setting).

As bleeding seems to mainly appear for fluid cement pastes, it seems reasonable to raise the issue of a correlation between fluidity and bleeding. This correlation is to be expected if one considers, on one hand, that bleeding, in the range of interest of industrial cementitious materials, cannot be described as the settlement of individual cement grains in a dilute system but rather as a consolidation process, i.e. the upward displacement of water through a compressible dense network of interacting cement grains [1–3]. On the other hand, it is now accepted that macroscopic flow of cement pastes is achieved as soon as the stress applied to the system overcomes what the network of interacting cement particles can support [4,5]. This flow onset defines what is called and measured as yield stress [4,5]. The interactions between cement grains are therefore at the origin of both yield stress of the material and grains network resistance to bleeding.

Moreover, from a practical point of view, a correlation between bleeding and yield stress could prove very handy as measurement of yield stress is easy whereas measurement of bleeding is delicate and time consuming. For instance, mini slump test is a cheap and fast method to assess the value of a given material yield stress [6–8]. Of course, yield stress of highly unstable cement pastes is difficult to access as the settling of particles quickly effects the measurement (especially under shear) but, in the case of interest (i.e. the cases in which bleeding is not obvious after a few minutes), being able to predict whether or not the material will bleed during the few hours before setting from a yield stress measurement carried out a few minutes after mixing should prove extremely valuable.

It may be however important to keep in mind that prediction of the evolution of a rheological or stability behavior over a few hours based on the first minutes behavior could be rather unrealistic in some cases. This would be the case in particular for cementitious systems, where aluminate reactivity is playing an important role and in which the adsorption or dispersion efficiency of a polymer in the system can vary over time.

We focus in this paper on a potential correlation between yield stress and bleeding. It has to be kept in mind that we do not try, in this paper, to model the bleeding phenomenon as in [1–3] but rather identify the conditions (i.e. the minimum yield stress value) under which it does not occur or can be neglected.

We suggest that the conditions under which the suspension is able to display a yield stress result from the competition between Brownian motion of the cement grains and colloidal interactions whereas the conditions under which the suspension is stable result from the competition between colloidal interactions and gravity. Therefore, the correlation between yield stress and bleeding is very indirect and difficult to use in practice.

* Corresponding author. Tel.: +33 1 4043 5285.
E-mail address: nicolas.roussel@lcpc.fr (N. Roussel).

0008-8846/$ – see front matter © 2012 Elsevier Ltd. All rights reserved.
doi:10.1016/j.cemconres.2012.03.015

2. Brownian motion, colloidal interactions and yield stress : theoretical frame

2.1. Brownian motion

Because of thermal agitation of the suspending fluid molecules, cement particles can undergo random (Brownian) motions, causing them to diffuse through the liquid. The level of energy associated to Brownian motion is typically of the order of kT where k is the Boltzmann constant and T the temperature in K. It was shown in [5] that, in steady state flows of standard cement pastes, Brownian motion can be neglected in front of the attractive colloidal interactions between cement grains. In systems containing high amounts of HRWRA in which the magnitude of the colloidal forces are severely reduced, it could however be imagined that Brownian forces could play a role in the behavior of the system.

2.2. Colloidal interactions

Several types of non-contact interactions occur within a cementitious suspension [4]. At short distance, cement particles interact via (generally attractive) van der Waals forces [9]. Also, there are electrostatic forces that result from the presence of adsorbed ions at the surface of the particles [10]. Polymer additives, present in many modern cementitious materials, can induce steric hindrance [11,12], which is believed to predominate over electrostatic repulsion. Each of these different interactions introduces non-contact forces between particles, the magnitude of which depends primarily on their separation distance.

Van der Waals interactions were shown to dominate all other colloidal interactions in the case of cement pastes and therefore dictate the inter-particle distance [9,13]. The inter-particle force is given by:

$$F \cong \frac{A_0 a^*}{12H^2} \tag{1}$$

where a^* is the radius of curvature of the "contact" points, H is the surface to surface separation distance at "contact" points and A_0 is the non retarded Hamaker constant [5].

When there are no polymers in the cement paste, the surface-to-surface separation distance at "contact" points H is estimated to be of the order of a couple nm [4,5]. When there are steric hindrances from adsorbed polymers, the surface-to-surface separation distance at "contact" points H is dictated by the conformation of the adsorbed polymer at the surface of the cement grains [13]. Orders of magnitude for typical polymers are around 5 nm [14]. It can be noted that recent advances have shown that it shall be possible to correlate the molecular structure of the polymer to its surface conformation [13].

2.3. Percolation volume fraction and the Yodel

In order to support a finite amount of stress without flow, the suspension must possess an internal network of interacting particles. An extreme situation occurs in very dilute suspensions (for large W/C) when particles (either individual or flocculated) are sufficiently far apart so that no percolated network is formed and the above-mentioned colloidal interactions are negligible. In this case, we must expect that the suspension is essentially Newtonian just as the water in which the particles are suspended. This situation was encountered in [15] where, above a critical value of W/C, the measured behavior of the tested cement pastes was purely Newtonian. The critical solid fraction value, below which the suspension does not have any yield stress, varies with the physicochemical properties of the cement powder and with the nature and amount of the additives used in the mixture. It can however be macroscopically defined as the percolation volume fraction ϕ_{perc}, above which a network of particles interacting through colloidal interactions appears in the material. Values ranging between 20 and 40% can be found in literature [16–18].

Recent progress on the prediction of yield stress from mix design for colloidal particles suspension has come from studies of the yield stress of metal oxide suspensions as a function of particles size, volume fraction of solids and pH [19,20]. A first principle analysis of yield stress has recently been proposed [17]. It successfully quantifies the main parametric dependencies observed experimentally by Zhou et al. [19,20] and can be extended to poly-disperse powder mixes [21]. The basic expression is written as:

$$\tau_0 \cong m \frac{A_0 a^*}{d^2 H^2} \frac{\phi^2 \left(\phi - \phi_{perc}\right)}{\phi_m (\phi_m - \phi)} \tag{2}$$

where m is a pre-factor, which depends on the particle size distribution, d is the particle average diameter, ϕ is the solid volume fraction and ϕ_m is the maximum packing fraction of the powder. This relation separates the contribution of the inter-particle force (Cf. Eq. (1)) and the contribution of the number of interacting particles, which depends on solid volume fraction. Giving the surface-to-surface separation distance the value of the adsorbed polymer layer between two particles allows the model to capture the fact that yield stress decreases with increasing adsorbed polymer layer thickness.

3. Materials and protocols

3.1. Tested materials and mixing procedure

A CEM I type cement of specific density 3.15 is used in this study. The Particle Size Distribution (PSD) was measured in ethanol using a laser particle size analyzer (Cf. Fig. 1). The specific surface measured using a Blaine apparatus of this cement is 3390 cm^2/g. The water to cement mass ratio (W/C) and admixture to cement ratio were chosen to cover the rheology range of cement pastes used in industrial practice. Yield stresses ranged therefore from 10 Pa to several hundred Pa.

The HRWRA used in this study is a commercial polycarboxylate type polymer. It is under liquid form containing 20% of dry material. Its recommended dosage ranges from 0.3 to 3% per weight of cement. The HRWRA is added to the mixing water before water/cement contact. Water is then mixed with cement in a planetary Hobart mixer. The mixing phase consists of two steps: 2 min at 140 rpm and 3 min at 280 rpm.

3.2. Polymer adsorption measurements

A Total Organic Carbon (TOC) analyzer is used in this work. The analysis technique involves a two-stage process commonly referred to as TC–IC. It allows for the measurement of both the amount of Inorganic Carbon (IC) by acidification of the sample and the amount

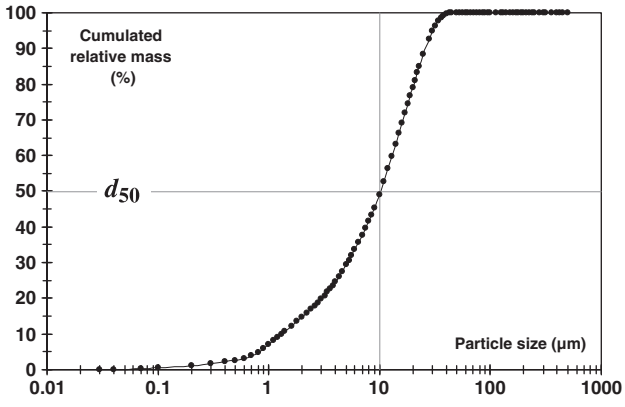

Fig. 1. Cement particle size distribution.

of Total Carbon (TC) in the sample. TOC is calculated by subtraction of the IC value from the TC of the sample. The TOC analyzer must first be calibrated with a cement paste sample in order to take into account the amount of organic carbon in cement due for instance to cement grinding agents. It can be noted that this amount is far from being neglectable and can strongly affect the measurements if left aside.

Cement pastes with a W/C ratio of 0.5 are centrifuged before TOC measurement. The centrifugation is carried out for 10 min at 5630 rpm in order to separate the liquid phase from the solid one. The liquid is then analyzed with the TOC analyzer. Furthermore, an analysis of the amount of organic carbon in reference solutions of polymer is carried out in order to calibrate the TOC analyzer. By comparison between the reference TOC value (TOC amount of polymer in reference polymer solution) and the "final" TOC (TOC amount of polymer in water extracted from cement paste), the amount of polymer adsorbed on mineral phases is computed.

3.3. Yield stress measurements

8 min after mixing, yield stress is measured using an Anton Paar Rheolab QC rheometer equipped with a Vane geometry. The measurement procedure is similar to the one used in Mahaut et al. [22]. After a one minute pre-shearing phase, a strain growth is applied to the sample at a shear rate of $0.001\ s^{-1}$ for 180 s. At such a low shear rate, viscosity effects are negligible and yield stress can be computed from the measured torque peak value at flow onset.

The vane geometry used in this study consists of four blades around a cylindrical shaft. For each measurement, the blade height and diameter are chosen among three geometries to improve the measurement accuracy. Tool geometries and maximal measurable yield stresses are given in Table 1.

It has to be kept in mind that, in the case of bleeding systems, the application of shear enhances the settling process and may lead to a high risk of misinterpretation. However, during the short duration of the tests carried out here, no bleeding was visually spotted.

In order to improve the reliability and accuracy of the experimental results, for each mixture, each yield stress measurement is performed six times on six different batches. This procedure allows for the computation of the experimental standard deviation value.

3.4. Bleeding measurements

After mixing, a 450 mm height and 30 mm diameter cylindrical tube made of transparent PVC is filled with cement paste. The initial height of the cement paste ranges from 250 to 300 mm for all tests. After filling, the tube is sealed to prevent any water evaporation. For each paste, bleeding water thicknesses are successively measured 60 min and 120 min after the end of the mixing phase.

4. Experimental results and analysis

4.1. Polymer adsorption

We plot in Fig. 2 the surface coverage ratio (i.e. the amount of adsorbed polymer divided by the amount of adsorbed polymer at the adsorption saturation plateau) as a function of the polymer dosage. An adsorption plateau seems to be reached for a polymer dosage higher than 2.5% of the cement mass. It can be noted that this dosage corresponds to the upper limit of the recommended dosage of the product.

Table 1
Vane geometries and maximum measurable yield stress for each geometry.

Tool	H (mm)	D (mm)	Maximum yield stress (Pa)
1	8.8	10	45 000
2	40	22	2200
3	60	40	400

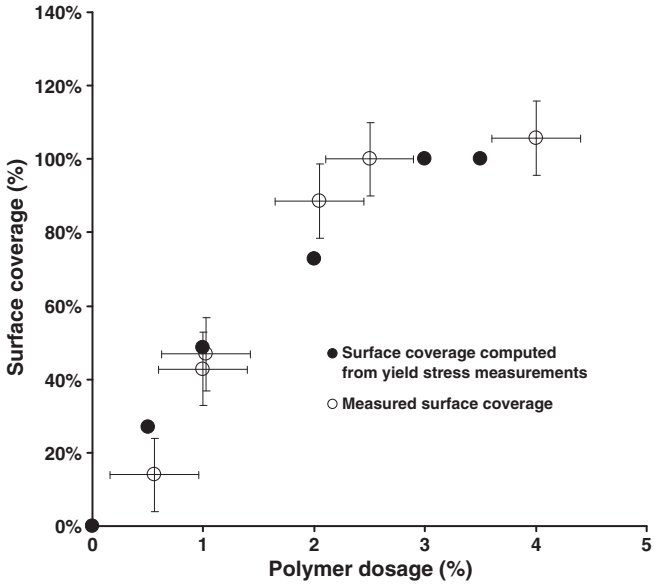

Fig. 2. Surface coverage ratio as a function of the polymer dosage.

4.2. Yield stress, percolation volume fraction and colloidal interactions

In Fig. 3, the measured yield stresses are plotted as a function of the solid volume fraction for dosages of HRWRA between 0 and 3%. The values range from a couple Pa to several hundreds of Pa. It can be noted that, above the saturation dosage obtained by adsorption measurements, the yield stress is not affected by polymer dosage.

The Flatt and Bowen YODEL (Eq. (2)) is also plotted in Fig. 3 for each tested mixture.

In order to compute Eq. (2), we consider here that the maximum packing fraction of the cement powder is 59%. This value was calculated using RENE LCPC [23] from the particle size distribution in Fig. 1. Moreover, for the sake of simplicity, we consider that the size of cement grains d is the average diameter d_{50} in Fig. 1 (i.e. 10 μm). The non retarded Hamaker constant value A_0 for C_3S is taken as $1.6\,10^{-20}$ J [5].

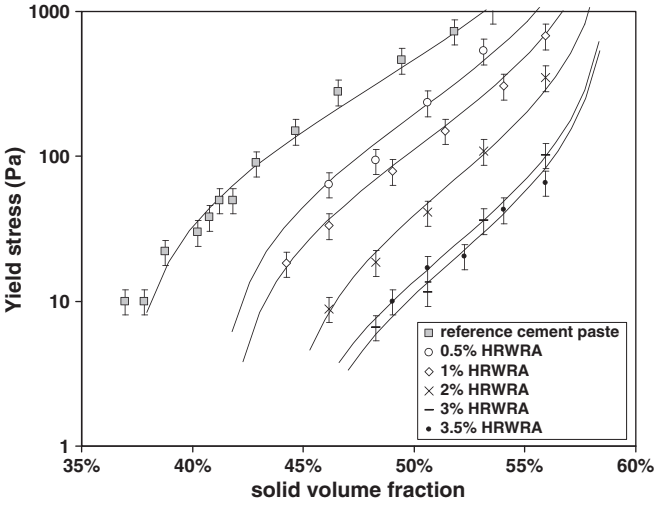

Fig. 3. Yield stress as a function of solid volume fraction for various HRWRA dosages. The solid lines are the predictions of the YODEL.

a^* is determined by the shape of the cement particles and not by their radius [17]. Its estimated value for cement particles is of the order of 300 nm [5].

There is a strong uncertainty on the value of the surface-to-surface separation distance in systems not containing any polymer that prevents the calibration of the model in this situation. There is moreover a strong possibility that the average interparticle force in absence of polymers is enhanced because of surface charge heterogeneity at the surface of the grains, which then disappear as added polymers preferably adsorbs on these heterogeneities. It seems therefore less misleading to calibrate the model at complete surface coverage.

The values for the polymer layer thickness that may be found in literature for polycarboxylate [13,14,17] are of the order of 5 nm. Using this value and fitting the Flatt and Bowen model to the experimental measurements for the mixtures at complete surface coverage, it is possible to obtain the value of m in Eq. (2). It is equal here to 40. We then use this value to predict the yield stress of all the other mixtures in Fig. 3, for which we fit the percolation volume fraction and the average surface-to-surface separation distance H. It can be noted that these parameters are fitted independently as the percolation volume fraction affects mainly the lowest values of the yield stress whereas the average surface to surface separation distance H imposes the divergence rate of the yield stress as volume fraction tends towards maximum packing fraction.

It can be seen in Fig. 3 that the YODEL is able to predict the yield stress of all mixtures for all dosages of HRWRA. Both experimental and computed results show that yield stress diverges for the maximal packing fraction of the powder for all mixtures. It can be noted that it is also the case for the mixture not containing any HRWRA, which is expected to be a highly flocculated system. This result is in contradiction with some traditional views of flocculated cement pastes as systems displaying an effective solid volume fraction higher than the real solid volume fraction because of water entrapped in the flocculated system [5,18].

The fitted values of H are plotted in Fig. 4. For the non admixed reference paste, the surface-to-surface separation distance is 1.5 nm and is very much in line with previous experimental results. It may be useful to stress that, as none of the other model parameters are fitted once the value of m is fitted on the cement paste at full surface coverage, obtaining the correct order of magnitude for the average surface-to-surface separation distance parameter is a convincing indication of the model ability to capture the underlying physics.

The value of H obtained for each dosage of HRWRA in Fig. 4 is an average value of the various surface-to-surface separation distances in the system. At full surface coverage, it is equal to two times the thickness of the adsorbed polymer layer H_p (i.e. 5 nm). Without any polymers, it is equal to two times an equivalent layer thickness H_0 at zero surface coverage. At intermediate surface coverage, it results from the contribution of the pairs of particles that do interact without any HRWRA, the pairs of particles that do interact via one adsorbed layer of HRWRA on one of the particles and the pairs of particles that do interact via one adsorbed layer of HRWRA on each of the particles.

From [24], it is possible to write that the average value of the various surface-to-surface separation distances in the system is a function of the surface coverage ratio θ, which dictates the statistical distribution of interactions:

$$\frac{1}{H^2} = \frac{\theta^2}{H_P^2} + \frac{8\theta(1-\theta)}{(H_P + H_0)^2} + \frac{(1-\theta)^2}{H_0^2} \tag{3}$$

It is possible to compute the surface coverage ratio from Eq. (3) and Fig. 4. The obtained values are plotted in Fig. 2. as a function of the polymer dosage.

The good agreement obtained between the values of surface coverage ratio computed from yield stress measurements and the surface coverage ratio measured independently by TOC analysis is again a convincing indication of the above models ability to capture the underlying physics and bring a link between macroscopic rheology and microscopic adsorption of polymers.

The fitted values of the percolation volume fraction are plotted in Fig. 5 as a function of HRWRA dosage. It can be seen that percolation volume fraction increases with HRWRA dosage. This result suggests that it is more difficult to create a stable network of interacting particles when the magnitude of the colloidal interaction energy is lower.

Recent advances on percolation volume fraction come from the numerical simulation of the Random Loose Packing (RLP) of slowly settling assemblies of interacting spheres [25] and allow us to go further in the analysis. It was demonstrated that, when particles are submitted to one interaction force F_i, which tends to prevent the particle from packing tightly, and one interaction force F_j, which tends to increase

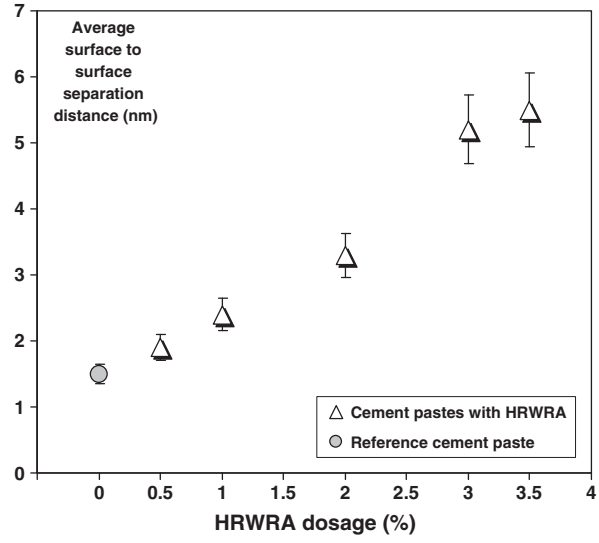

Fig. 4. Average surface-to-surface separation distance as a function of the HRWRA dosage.

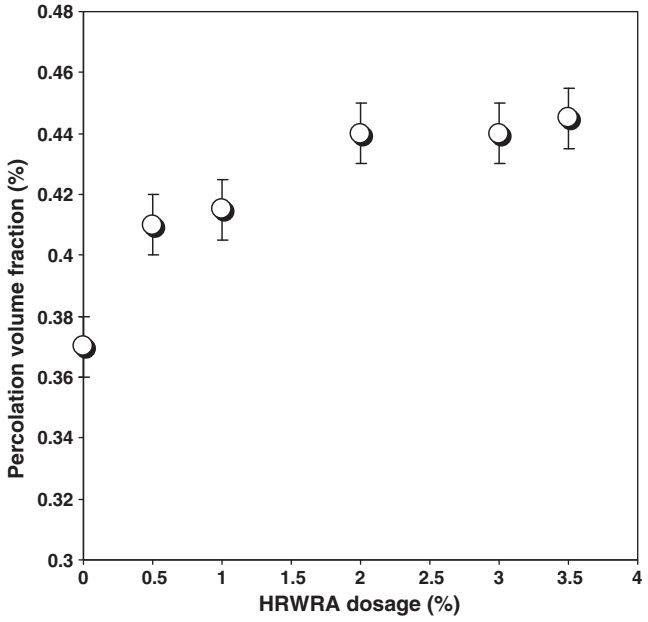

Fig. 5. Percolation volume fraction as a function of the HRWRA dosage.

the packing of the particles, the relative magnitude of the two forces imposes the minimal packing fraction φ_{RLP} of the stable network that can be formed by the particles with

$$\phi_{RLP} = \phi_m\left(1-\exp\left(-2.457\chi^{-0.212}\right)\right) \quad (4)$$

where ϕ_m is the maximum packing fraction of the particles and $\chi = F_i/F_j$ is the interaction forces ratio [25].

When considering the percolation volume fractions in Fig. 5, it can be assumed that the two forces acting on particles, in this specific case, are, on one hand, the colloidal attractive Van der Waals forces, which tend to bring the particles together and form a network able to withstand a stress and, on the other hand, the Brownian forces, which tend, through random agitation, to disrupt this interaction network. The attractive Van der Waals force is given by Eq. (1) ($F \cong A_0 a^*/12H^2$) whereas the force associated to Brownian motion can be dimensionally estimated as kT/d (Cf. Section 2.1). For a given amount of HRWRA, the surface-to-surface separating distance can then be extracted from Fig. 4. The minimal packing fraction ϕ_{perc} of the stable network that can be formed by the particles can then be calculated using Eq. (4) and 59% as the maximum packing fraction of the cement grains (Cf. Fig. 6). Below ϕ_{perc}, there are not enough particles in the system to create an interaction network able to resist Brownian agitation. It could be expected that, in this regime, the system rheological behavior shall be Newtonian. We will however show further in this work that these systems are unstable and settle [26]. Above ϕ_{perc}, there are enough particles in the system to create an interaction network able to resist Brownian agitation. The system has a yield stress that can be predicted using Eq. (2). ϕ_{perc} is plotted in Fig. 6 as a function of the surface-to-surface separating distance and compares well with the values computed from the experimental yield stress measurements.

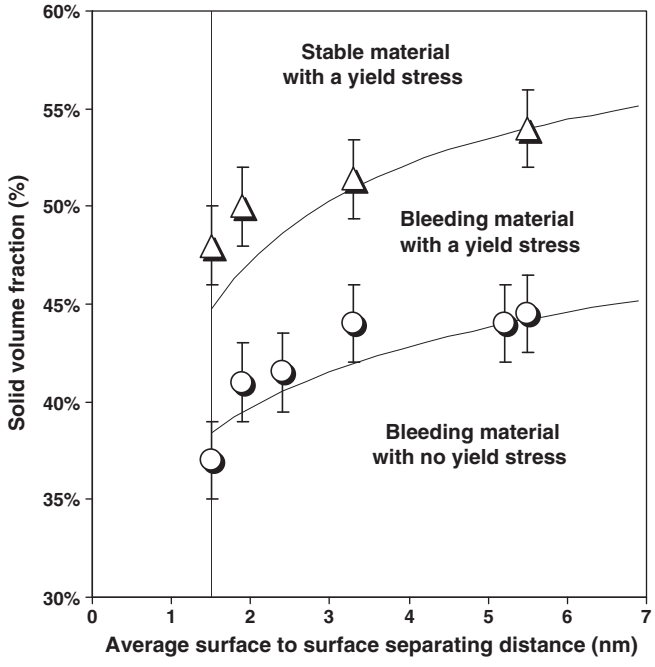

Fig. 6. Percolation and stability solid volume fractions as a function of the average surface-to-surface particle separating distance. The circles are the percolation volume fraction above which the suspension displays a yield stress whereas the triangles are the stability volume fractions above which the material is stable and does not bleed. The two continuous curves are theoretical predictions (Cf. text for more details).

4.2. Bleeding

As described in Section 3.3, bleeding water thicknesses were successively measured 60 min and 120 min after the end of the mixing phase. The results are plotted in Fig. 7 for different dosages of HRWRA.

It can be seen that, as soon as some bleeding is measured at 60 min, it either increases at 120 min or stays constant. Moreover, when bleeding water thickness increases at 120 min, bleeding rate seems however to decrease.

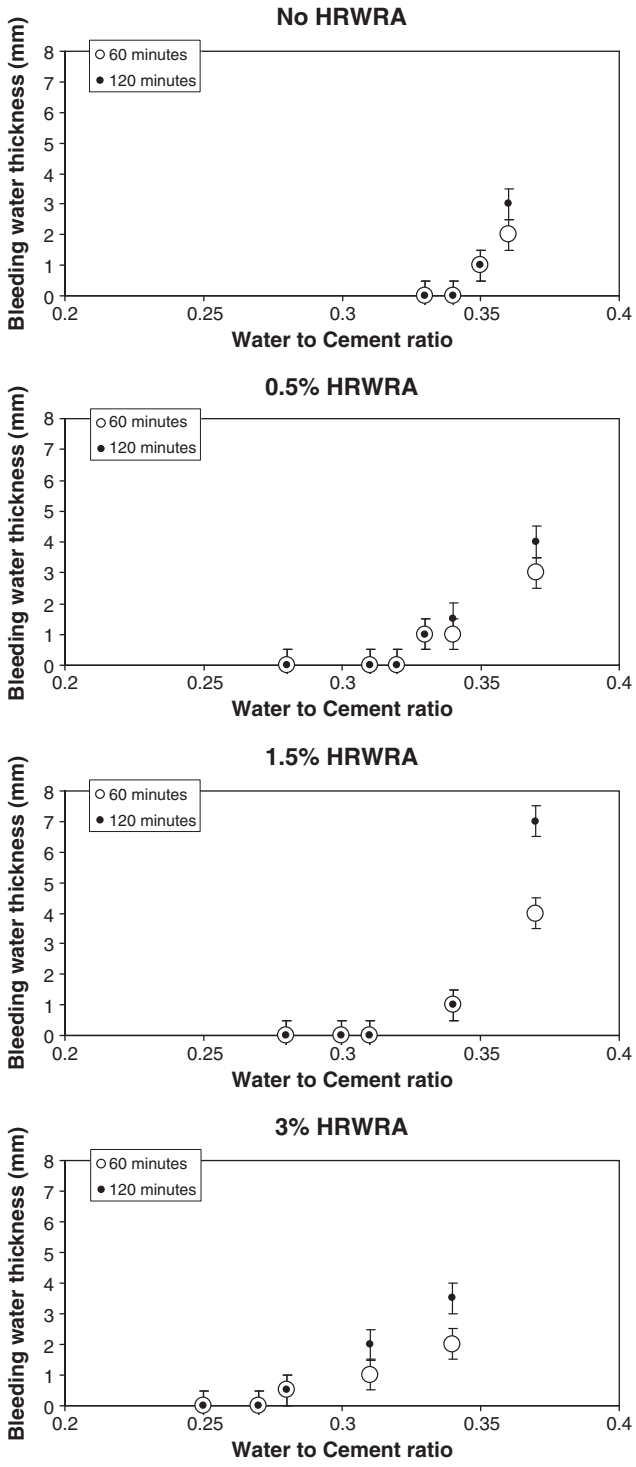

Fig. 7. Bleeding water thickness as a function of the water to cement ratio for various HRWRA dosages.

We focus here on the fact that there exists in Fig. 7 for each HRWRA dosage a critical water to cement ratio for which no bleeding is measured. Below this critical ratio, the material seems to be stable. This feature was also spotted in [27], in which the authors introduced a critical HRWRA dosage, above which sedimentation occurred. This dosage was shown to be dependent on the solid volume fraction. We checked that this critical ratio did not depend on the height of the paste column in the cylindrical tube. We measured the bleeding thickness after 120 min for three different heights (20 cm, 30 cm and 40 cm). We plot in Fig. 8 the evolution of the bleeding water thickness as a function of the water to cement ratio for these different heights. When the material is unstable, the bleeding rate increases with the sample height as it depends on the pressure gradient at the origin of water extraction, which itself depends on the height of the sample. However, the measured critical water to cement ratio under which the material is stable does not depend on the sample height, showing that its origin lies in a local equilibrium between particle interactions (number and intensity) and gravity.

If we were interested here in the prediction of the bleeding process, we would then describe either the viscous drag force on cement particles or, keeping in mind the high solid volume fraction of these systems, introduce permeability and Darcy's law for the cement grains assembly [1–3]. More accurate approaches would even take into account the fact that the permeability of the cement grains assembly decreases as water leaves the system [1,2,28,29] following a consolidation process. Either technique would allow for the accounting of the influence of the viscous nature of the interstitial fluid on the bleeding rate. However, as we are only interested here in predicting whether or not bleeding shall occur, we are not interested in time effect. We therefore focus on the dominating driving phenomenon. Therefore, in a non-thixotropic cement paste, if colloidal inter-particle forces are able to resist gravity, there shall not be any bleeding. If gravity dominates colloidal forces, bleeding shall occur.

We plot in Fig. 9 the above stability water to cement ratio as a function of the HRWRA dosage. It can be noted that, as it was the case when Brownian agitation was threatening the stability of the interaction network, it is more difficult to create a network of interacting particles able to resist gravity when the magnitude of the colloidal interaction energy decreases.

As in the previous section, we use here Eq. (4) to predict the minimal solid volume fraction $\phi_{RLP}^{bleeding}$ that can be formed by the particles to resist gravity. The two forces acting on particles are now, on one hand, the colloidal attractive Van der Waals forces, which tend to bring the particles together and form a network able to resist gravity and, on the other hand, gravity, which tends to deform this interaction network and increases packing. As before, the attractive Van der Waals force is given by Eq. (1) ($F \cong A_0 a^*/12H^2$) whereas the force associated to gravity can be estimated as $\Delta\rho g\pi d^3/6$. As before, for a given amount of HRWRA, the surface-to-surface separating distance can be extracted from Fig. 4. Below $\phi_{RLP}^{bleeding}$, there are not enough particles in the system to create an interaction network able to resist gravity. It can be noted that the separating force associated to gravity (of the order of 10^{-11} N) is always several orders of magnitude higher than the force associated to Brownian motion (of the order of 10^{-15} N). As a consequence, Brownian motion cannot stabilize the suspension and prevent settling of cement particles. It has to be kept in mind that we only consider here an average diameter of 10 μm. In the case of the smallest particles (i.e. lower than 500 nm), in the case where they are not flocculated, Brownian agitation and gravity have the same order of magnitude and these particles could be stable in water affecting the color of the bleeding water [26]. Above $\phi_{RLP}^{bleeding}$, there are enough particles in the system to create an interaction network able to resist gravity and no bleeding is measured. $\phi_{RLP}^{bleeding}$ is plotted in Fig. 6 as a function of the average surface-to-surface separating distance imposed by the HRWRA and compares well with the values computed from the experimental bleeding measurements.

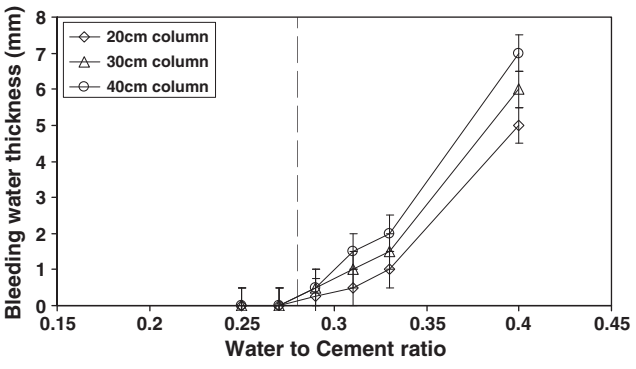

Fig. 8. Bleeding water thickness as a function of the W/C ratio for various column heights.

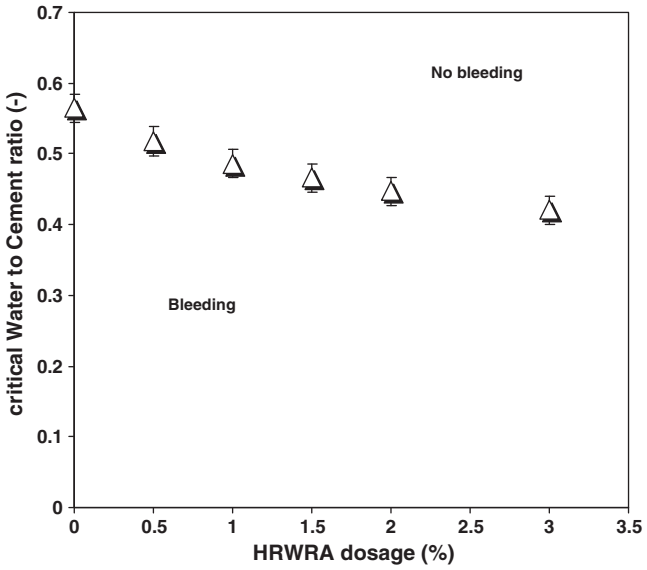

Fig. 9. Critical water to cement ratio below which the cement paste does bleed as a function of the HRWRA dosage.

Because of the focus given here to a stability criterion, the present approach shall not be able to describe, for instance, the effect of viscosity agents, which thicken the interstitial fluid and slow down the bleeding phenomenon [30]. In this latter case, competition between gravity and colloidal forces could be unchanged by the viscosity agent but the decrease in interstitial fluid mobility would slow down the settling process. The decrease in bleeding rate induced by this type of admixture could therefore reduce the practical consequences of bleeding and make them neglectable from an industrial point of view.

We moreover do not account for very specific systems such as self-leveling floor screed, which are both very thixotropic and chemically accelerated. In this latter case, structural build up [31–33], CSH early nucleation between cement grains and fast rigidification of the paste due to high chemical activity [34,35] could play a non neglectable role on the stabilization of cement grains [36].

It can be noted that, at the critical solid volume fraction above which no bleeding is measured, the yield stresses of the tested cement pastes are between 300 Pa for the cement paste not containing any HRWRA and 40 Pa for the cement paste containing 3% HRWRA (Cf. Fig. 10). This shows that there is no direct correlation between bleeding and yield stress although both properties are strongly linked with the magnitude of the colloidal interactions and the volume fraction of the suspension.

It moreover stresses the fact that, as these yield stresses are rather high and prevent or at least penalizes the mix design of fluid materials

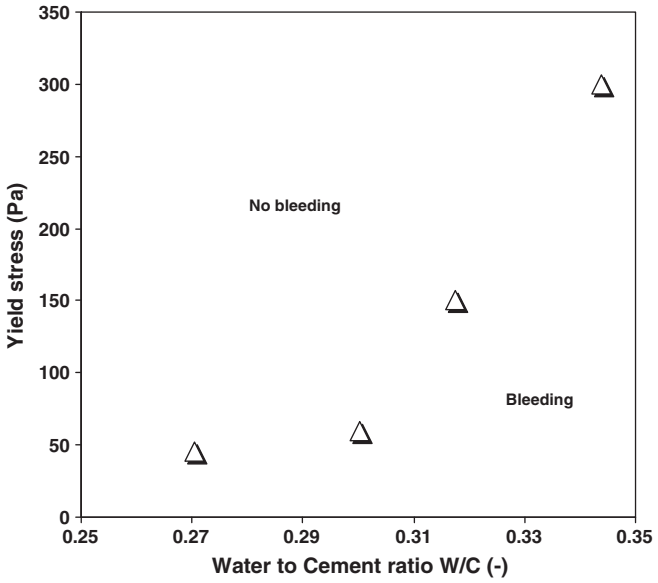

Fig. 10. Critical value of the yield stress for which the paste does not display any bleeding as a function of the water to cement mass ratio W/C.

such as Self Compacting Concrete, knowledge on viscosity modifying agents and exact prediction of bleeding as a function of time before setting are needed in industrial practice.

5. Concluding general frame

We neglected in this paper any consequences of cement hydration and recalled that three physical phenomena are acting simultaneously in a fresh cement paste at rest:

- *Brownian motion* which only depends on temperature,
- *colloidal attractive forces*, which depend on the average distance between interacting particles (which itself depends on the polymer conformation at the surface of the cement grain). Their collective macroscopic impact on rheology depends on the number of interacting particles (i.e. solid volume fraction) and on polymer surface coverage.
- *gravity*, the consequences of which mainly depends on the grain average diameter.

If *colloidal attractive forces* dominate *Brownian motion*, which is the case for most cementitious materials in industry, a percolated network of interacting particles appears within the suspension. It is able to withstand an external stress up to a critical value called yield stress. A recently developed model can predict this critical value: the YODEL. It is severely affected by solid volume fraction and, for a given polymer, by polymer surface coverage. At saturation (i.e. when it does not depend on surface coverage), it only depends on the conformation of the polymer adsorbed at the surface of the cement grain. This conformation imposes the surface-to-surface separation distance.

If *Brownian motion* dominates *colloidal attractive forces* (in the case of diluted systems or systems at high admixture concentration), the suspension does not have any yield stress. The network of attractive colloidal interactions is instantaneously destroyed by the Brownian agitation and is not able to withstand any external stress. In this particular case, it could be imagined that *Brownian motion* dominates *gravity*. The result would be a stable Newtonian viscous suspension. However, according to the order of magnitudes of the two phenomena, this cannot happen in the case of typical cementitious materials. Suspensions, in which Brownian motion dominates colloidal forces, shall always therefore be unstable and display high levels of bleeding.

If *colloidal attractive forces* dominate *gravity*, particles are trapped in the colloidal interactions network and are therefore not able to rearrange their relative positions. The suspension is stable. There is no bleeding and the fresh cement pastes stays homogeneous.

If *gravity* dominates *colloidal attractive forces*, particles may settle. This induces a relative displacement of the cement particles within the interstitial fluid or a relative displacement of the interstitial fluid between the cement particles. This phenomenon is time driven and is influenced by the viscosity of the interstitial fluid (which can be affected by viscosity agents) and the permeability of the porous medium formed by the interacting cement grains (which mainly depends on the solid volume fraction and on the average diameter of the grains). Within very specific conditions, bleeding may be adequately limited by the above mix design factors. It is in this regime only that fluid cement pastes allowing for the production of fluid concrete can be mix designed.

Acknowledgment

Authors would like to acknowledge the European Community for its financial support and Prof. Robert Flatt for the very fruitful discussions.

References

[1] L. Josserand, O. Coussy, F. de Larrard, Bleeding of concrete as an ageing consolidation process, Cem. Concr. Res. 36 (2006) 1603–1608.
[2] T.S. Tan, T.H. Wee, S.A. Tan, C.T. Tam, S.L. Lee, A consolidation model for bleeding of cement paste, Adv. Cem. Res. 1 (1987) 18–26.
[3] C.A. Clear, D.G. Bonner, Settlement of fresh concrete — an effective stress model, Mag. Concr. Res. 40 (142) (1988 March) 3–12.
[4] R.J. Flatt, Towards a prediction of superplasticized concrete rheology, Mater. Struct. 27 (2004) 289–300.
[5] N. Roussel, A. Lemaître, R.J. Flatt, P. Coussot, Steady state flow of cement suspensions: a micromechanical state of the art, Cem. Concr. Res. 40 (2010) 77–84.
[6] N. Roussel, C. Stefani, R. Leroy, From mini cone test to Abrams cone test : measurement of cement based materials yield stress using slump tests, Cem. Concr. Res. 35 (5) (2005) 817–822.
[7] N. Roussel, Rheology of fresh concrete: from measurements to predictions of casting processes, Mater. Struct. 40(10) (2007) 1001–1012.
[8] N. Roussel, P. Coussot, "Fifty-cent rheometer" for yield stress measurements: from slump to spreading flow, J. Rheol. 49 (3) (2005) 705–718.
[9] R.J. Flatt, Dispersion forces in cement suspensions, Cem. Concr. Res. 34 (2004) 399–408.
[10] R.J. Flatt, P. Bowen, Electrostatic repulsion between particles in cement suspensions: domain of validity of linearized Poisson–Boltzmann equation for non-ideal electrolytes, Cem. Concr. Res. 33 (2003) 781–791.
[11] P.F.G. Banfill, A discussion of the paper "Rheological properties of cement mixes" by M. Daimon and D.M. Roy, Cem. Concr. Res. 9 (1979) 795–798.
[12] K. Yoshioka, E. Sakai, M. Daimon, A. Kitahar, Role of steric hindrance in the performance of superplasticizers in concrete, J. Am. Ceram. Soc. 80(10) (1997) 2667–2671.
[13] R.J. Flatt, I. Schober, E. Raphael, C. Plassard, E. Lesniewska, Conformation of adsorbed comb copolymer dispersants, Langmuir 25 (2) (2009) 845–855.
[14] A.M. Kjeldsen, R.J. Flatt, L. Bergström, Relating the molecular structure of comb-type superplasticizers to the compression rheology of MgO suspensions, Cem. Concr. Res. 36 (2006) 1231–1239.
[15] L. Struble, G.K. Sun, Viscosity of Portland cement pastes as a function of concentration, Adv. Cem. Based Mater. 2 (1995) 62–69.
[16] Z. Toutou, N. Roussel, Multi scale experimental study of concrete rheology: from water scale to gravel scale, Mater. Struct. 37 (2) (2006) 167–176.
[17] R.J. Flatt, P. Bowen, Yodel: a yield stress model for suspensions, J. Am. Ceram. Soc. 89 (4) (2006) 1244–1256.
[18] S. Mansoutre, P. Colombet, H. Van Damme, Water retention and granular rheological behaviour of fresh C3S paste as function of concentration, Cem. Concr. Res. 29 (1999) 1441–1453.
[19] Z. Zhou, M.J. Solomon, P. Scales, D.V. Boger, The yield stress of concentrated flocculated suspensions of size distributed particles, J. Rheol. 43 (1999) 651–671.
[20] Z. Zhou, P.J. Scales, D.V. Boger, Chemical and physical control of the rheology of concentrated metal oxide suspensions, Chem. Eng. Sci. 56 (2001) 2901–2920.
[21] R.J. Flatt, P. Bowen, Yield stress of multimodal powder suspensions: an extension of the YODEL (Yield Stress mODEL), J. Am. Ceram. Soc. 90 (4) (2007) 1038–1044.
[22] F. Mahaut, S. Mokeddem, X. Chateau, N. Roussel, G. Ovarlez, Effect of coarse particle volume fraction on the yield stress and thixotropy of cementitious materials, Cem. Concr. Res. 38 (2008) 1276–1285.
[23] F. de Larrard, Concrete Mixture Proportioning, E & FN Spon, London, 1999.

[24] R. Flatt, I. Schober, Superplasticizers and the rheology of concrete, in: N. Roussel (Ed.), Understanding the Rheology of Concrete, Woodhead Publishing, 2012.
[25] K.J. Dong, R.Y. Yang, R.P. Zou, A.B. Yu, Role of interparticle forces in the formation of random loose packing, Phys. Rev. Lett. 96 (2006) 145505.
[26] C.M. Neubauer, M. Yang, H.M. Jennings, Interparticle potential and sedimentation behaviour of cement suspensions: effects of admixtures, Adv. Cem. Based Mater. 8 (1998) 17–27.
[27] R.J. Flatt, Y.F. Houst, P. Bowen, H. Hoffmann, J. Widmer, U. Sulser, U. Maeder, T.A. Bürge, Effect of superplasticizers in a highly alkaline model suspensions containing silica fume, in: V.M. Malhotra (Ed.), Proc. 6th Canmet/ACI Int. Conf. Fly-Ash, Silica Fume, Slag and Natural Pozzolans in Concrete, American Concrete Institute, Detroit, 1998, pp. 911–930, SP-178.
[28] P.H. Morris, P.F. Dux, Analytical solutions for bleeding of concrete due to consolidation, Cem. Concr. Res. 40 (2010) 1531–1540.
[29] V. Picandet, D. Rangeard, A. Perrot, T. Lecompte, permeability measurement of fresh cement paste, Cem. Concr. Res. 41 (2011) 330–338.
[30] Kamal H. Khayat, Viscosity-enhancing admixtures for cement-based materials — an overview, Cem. Concr. Compos. 20 (1998) 171–188.
[31] P. Billberg, development of SCC static yield stress at rest and its effect on the lateral form pressure, in: S.P. Shah (Ed.), Proceedings of the Second North American Conference on the Design and use of Self-Consolidating Concrete and the Fourth International RILEM Symposium on Self-Compacting Concrete, October 30–November 3 2005, Chicago, USA, 2005.
[32] N. Roussel, Steady and transient flow behaviour of fresh cement pastes, Cem. Concr. Res. 35 (2005) 1656–1664.
[33] N. Roussel, A thixotropy model for fresh fluid concretes: theory, validation and applications, Cem. Concr. Res. 36 (2006) 1797–1806.
[34] L. Nachbaur, J.C. Mutin, A. Nonat, L. Choplin, Dynamic mode rheology of cement and tricalcium silicate pastes from mixing to setting, Cem. Concr. Res. 31 (2001) 183–192.
[35] N. Roussel, G. Ovarlez, S. Garrault, C. Brumaud, The origins of thixotropy of fresh cement pastes, Cem. Concr. Res. 42 (2012) 148–157.
[36] F. Rosquoet, A. Alexis, A. Khelidj, A. Phelipot, Experimental study of cement grout: rheological behavior and sedimentation, Cem. Concr. Res. 33 (2003) 713–722.